ARTICLE

Microphase Separation in A_2B Copolymer Melts

Xiao-yan Yan, Hao-jun Liang*

Department of Polymer Science and Engineering, University of Science and Technology of China, Hefei 230026, China

(Dated: Received on April 4, 2006; Accepted on September 7, 2006)

The microphase diagrams of special A_2B copolymer melts were presented by using the self-consistent field theory for star copolymer systems. Unlike the phase diagram of diblock copolymer, only three classical structures, namely spherical phase, cylindrical phase and lamellar phase were discovered in the diagram of the A_2B system. The change in chain architectures allowed sufficient shifts of phase boundaries and widened the range of f_B for which lamellar phase occurred, to some degree. Simply, an asymmetric architecture for copolymer allowed control of the morphology independent of the volume fraction.

Key words: Y copolymer, Self-consistent field theory, Microstructure, Phase diagram, Boundaries shift

I. INTRODUCTION

Block copolymers are versatile in their abilities to show a menagerie of morphologies as a function of the relative lengths of the blocks and the temperature (or the magnitude of χN, where χ is the Flory interaction parameter and N is the degree of polymerization) [1,2]. The variations of composition, architecture and choice of monomers can lead to dramatic changes in self-assembly at the mesoscale and, consequently, in properties. For example, commercial materials based on blocks of polystyrene and polybutadiene have properties that vary from high modulus, tough thermoplastics to soft, highly extensible thermoplastic elastomers [3]. Due to the potential applications of polymers in their self-assembly, the microstructures and properties of polymers have been extensively researched both in simulation [4,5] and in experiment [6].

Theoretical advances in past years have greatly improved our understanding of the connection between copolymer architecture and self-assembly behavior in diblock melts. As provided by Helfand in the late 1970s [7], the relationship between block copolymer composition and the thermodynamic stability of the lamellar, cylindrical, and spherical phases was firmly established. In the 1980s, Leibler, Semenov and others further developed the analytical machinery to do such calculations [8,9]. Several decades of research culminated in broad agreement between the experimental observations and the phase diagram calculated by self-consistent field theory (SCFT) by Matsen and Schick [10], in the mid 1990s. The resulting phase diagram contains four types of structures: body-centered-cubic spheres, hexagonally ordered cylinders, lamella, and gyroid [11]. The O^{70} network is found to be stable within a narrow window that overlaps the low χN end of the region [12].

Self-consistent field theory (SCFT) for copolymer melts has now been highly successful in describing complex morphologies in block copolymers. An ABC starblock copolymer system has been calculated and its phase diagram has been predicted by Yang, on a 2D lattice [13]. Furthermore, calculations for $(AB)_m$ starblock copolymers have also demonstrated modest compositional shifts of phase boundaries for practical values of the number of starblock arms [14]. More complex copolymers were researched by Milner for A_nB_m copolymers ($n \neq m$) [15] and Fredrickson for AB_n copolymers [16]. In an A_nB_m copolymer system, n A blocks and m B blocks are connected at a central junction point, and much more substantial shifts of phase boundaries were also predicted. In this work, the functional dependence between the microphase of Y copolymers and the relative lengths of the blocks was calculated using the self-consistent mean field theory, then the phase diagram was contrasted with that of diblock copolymers.

II. SIMULATION

We consider a system of n A_2B copolymers each of polymerization, N, in volume V. Components A and B consist of $f_A N$ and $f_B N$ ($f_B = 1 - f_A$) while the A_1 and A_2 blocks consist of $f_{A_1} N$ and $f_{A_2} N$ ($f_{A_2} = f_A - f_{A_1}$), respectively. In real-space SCFT, one considers the statistics of a single copolymer chain in a set of effective chemical potential fields ω_I, where I can represent block A_1, A_2 or B. These chemical potential fields which replace the actual interactions between different components are conjugated to the segment density fields, ϕ_I, of block segment I. Each polymer block is parameterized with the variable s which increases along each arm. The core of the star corresponds to $s=0$. Along each arm, s increases from 0 at the core to $f_I N$ at the outer end. With these definitions, the polymer

*Author to whom correspondence should be addressed. E-mail: hjliang@ustc.edu.cn, senrd@vip.sina.com

segment probability distribution functions $q_I(\vec{r},s)$ and $q'_I(\vec{r},s)$ for species I satisfy the modified diffusion equation [17,18]:

$$\frac{\partial q_I(\vec{r},s)}{\partial s} = \frac{a^2}{6}\nabla^2 q_I(\vec{r},s) - \omega_I(\vec{r})q_I(\vec{r},s) \quad (1)$$

$$\frac{\partial q'_I(\vec{r},s)}{\partial s} = -\frac{a^2}{6}\nabla^2 q'_I(\vec{r},s) + \omega_I(\vec{r})q'_I(\vec{r},s) \quad (2)$$

where a is the Kuhn length of the polymer segment, and $0 < s < f_I N$. The initial conditions are $q_I(\vec{r},0) = \prod_{k\neq I} q'_k(\vec{r},f_k N)$, where $k \in \{\mathrm{A}_1, \mathrm{A}_2, B\}$ and $q'_I(\vec{r},f_I N) = 1$. Note that one must solve for $q'_I(\vec{r},s)$ prior to solving for $q_I(\vec{r},s)$. Accordingly, the partition function of a single chain subjected to the mean field $\omega_I(\vec{r})$ can be written as $Q = \int \mathrm{d}r q_I(\vec{r},s)q'_I(\vec{r},s)$ in terms of $q_I(\vec{r},s)$ and $q'_I(\vec{r},s)$, and Q is independent of the contour length parameter of a chain s. The equation for Q may be rewritten as

$$Q = \frac{1}{V}\int \mathrm{d}\vec{r} q_I(\vec{r},f_I N) \quad (3)$$

Hence, the free energy function of the system is given by [19]

$$\widetilde{F} = -\ln Q(\omega_\mathrm{A},\omega_\mathrm{B}) + \frac{1}{V}\int \mathrm{d}r[\chi N(\phi_\mathrm{A}-\bar{\phi}_\mathrm{A})(\phi_\mathrm{B} - \bar{\phi}_\mathrm{B}) - \omega_A\phi_\mathrm{A} - \omega_\mathrm{B}\phi_\mathrm{B} - P(1-\phi_\mathrm{A}-\phi_\mathrm{B})] \quad (4)$$

where N is the length of the copolymer chain, χ_{ij} is the Flory-Huggins interaction parameter between species i and j, and $\bar{\phi}_\mathrm{A}(\bar{\phi}_\mathrm{B})$ is the average volume fraction of the A[B] species. The field P is a "pressure field" introduced to enforce incompressibility, also known as a Lagrange multiplier. The value of the fields $[\phi_\mathrm{A},\phi_\mathrm{B},\omega_\mathrm{A},\omega_\mathrm{B},P]$ at the saddle-point satisfies the following set of equations that describe the equilibrium morphology:

$$\omega_\mathrm{A}(\vec{r}) = \chi N[\phi_\mathrm{B}(\vec{r}) - \bar{\phi}_\mathrm{B}] + P(\vec{r}) \quad (5)$$

$$\omega_\mathrm{B}(\vec{r}) = \chi N[\phi_\mathrm{A}(\vec{r}) - \bar{\phi}_\mathrm{A}] + P(\vec{r}) \quad (6)$$

$$\phi_\mathrm{A}(\vec{r}) + \phi_\mathrm{B}(\vec{r}) = 1 \quad (7)$$

$$\phi_{\mathrm{A}_1}(\vec{r}) = \frac{V}{Q}\int_0^{f_{\mathrm{A}_1}N} \mathrm{d}s q_{\mathrm{A}_1}(\vec{r},s)q'_{\mathrm{A}_1}(\vec{r},s) \quad (8)$$

$$\phi_{\mathrm{A}_2}(\vec{r}) = \frac{V}{Q}\int_0^{f_{\mathrm{A}_2}N} \mathrm{d}s q_{\mathrm{A}_2}(\vec{r},s)q'_{\mathrm{A}_2}(\vec{r},s) \quad (9)$$

$$\phi_\mathrm{B}(\vec{r}) = \frac{V}{Q}\int_0^{f_\mathrm{B}N} \mathrm{d}s q_\mathrm{B}(\vec{r},s)q'_\mathrm{B}(\vec{r},s) \quad (10)$$

We solve Eq.(5) to Eq.(10) directly in real space by using a combinatorial screening algorithm proposed by Drolet and Fredrickson [20,21]. The algorithm consists of randomly generating the initial values of $\omega_I(\vec{r})$. Using a Crank-Nicholson scheme and the alternating-direct implicit method [22], we integrate the diffusion equations to obtain q and q' for $0 < s < f_I N$. Then, Eqs.(8)-(10) are evaluated to obtain new expression values for the volume fractions of blocks A and B. The effective pressure field P in Eq.(5) and Eq.(6) can be calculated as $P^{n+1}=({\omega_\mathrm{A}}^{n+1}+ {\omega_\mathrm{B}}^{n+1})/2$. The chemical potential field ω_I can be updated by using the equations

$${\omega_I}^{\mathrm{new}} = {\omega_I}^{\mathrm{old}} + \Delta t\frac{\delta F}{\delta \phi_I} \quad (11)$$

$$\frac{\delta F}{\delta \phi_I} = \sum\nolimits_{M\neq I}\chi_{IM}[\phi_M(r) - f_M] + P(r) - {\omega_I}^{\mathrm{old}} \quad (12)$$

as the chemical potential force. The above steps are iterated until the free energy converges to a local minimum, where the phase structure corresponds to a metastable state. This iteration scheme is a pseudo-dynamic process with the steepest descent on the energy landscape to the nearest metastable solution. It is possible to reach various metastable states depending on the initial conditions. We also minimize the free energy with respect to the system size because it has been pointed out that the box size can influence the morphology, and use different initial conditions. Therefore, by varying the volume fraction of compositions and the interaction parameters systematically, we can obtain not only the typical morphologies but also the phase diagram.

The simulations were carried out in a $25 \times 25 \times 25$ cube with periodic boundary conditions, space length L= 6.25 and grid size Δx=0.25 in the unit of R_g (unperturbed mean-square radius-of-gyration of a copolymer chain). The simulations for each sample are carried out until the phase patterns are stable and invariable with time and $\Delta F < 10^{-8}$. In this paper, we present a Y copolymer system, which consists of two segments of A monomers and one segment of B monomers by grafting B blocks onto the center of an A block backbone. A sketch map of this Y copolymer is given in Fig.1.

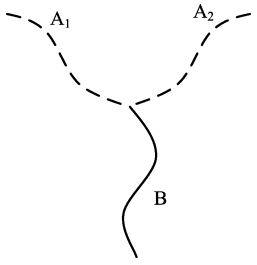

FIG. 1 Schematic picture of the A_2B star copolymers. The B block is connected at the middle of the A block.

III. RESULTS AND DISCUSSION

Firstly, the microphase behavior of AB diblock copolymers was studied by ranging χN from the order-

ISSN 1003-7713/DOI:10.1360/cjcp2007.20(1).43.5

disorder transition (ODT) to the intermediate segregation regime. The spherical structure (S) (Fig.2(a)), hexagonal-packed cylindrical structure (C) (Fig.2(b)), perforated lamellar structure (PL) (Fig.2(c)), and lamellar structure (L) (Fig.2(d)) were discovered. Figure 3 shows the phase boundaries of all the above microstructures, which are almost identical to the results given in Ref.[7], especially when $\chi N<20$. However, we found only a perforated lamellar structure in the C-L transition region where Matsen has predicted the gyroid phase would occur. This perforated lamella has been proven to be an unusually long-lived nonequilibrium structure involved in the formation of the gyroid phase [23] which can always be transformed into the gyroid phase under appropriate circumstances [24]. Due to the limits of SCFT and the instability of microphase transitions, we could not determine accurate boundaries of the cylindrical and lamellar structures. Nonetheless, we can present the approximate boundaries of the above several phases so that we can investigate the dependence of self-assembly on the chain architecture.

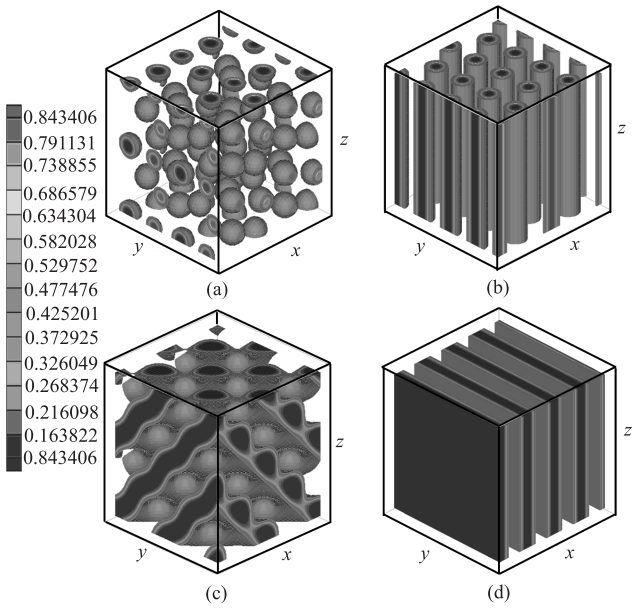

FIG. 2 Four examples of microstructures are (a) spheres of A, f_B=0.83 with χN=30; (b) hexagonal-packed cylinders of A, f_B=0.72 with χN=18; (c) perforated lamella of B, f_B=0.62 with χN=30; (d) lamella, f_B=0.5 with $\chi N = 20$.

Secondly, we studied the self-assembly of Y copolymer system and present its phase diagram by exploring χN in the parameter space as with the AB linear diblock copolymer. There are two notable aspects in the morphology diagram of the Y copolymer. One is that only three ordered microstructures, namely body-centered-cubic spheres (S), hexagonally packed cylinders (C) and lamella (L), were discovered. The other is that sufficient boundary shifts can be found relative to the diagram of diblock copolymer. The morphological behavior of a series of well-defined A_2B graft block copolymers has been studied by Pochan and Gido [25]. This model architecture is formed by grafting a polystyrene block onto the center of a polyisoprene backbone. In their experiment, the I_2S copolymer was observed to form lamellar microstructure at f_S=0.62, and the hexagonally packed PS cylinders in a PI matrix were discovered at f_S=0.31. In Fig.3, we can also see the lamellar phase and hexagonally packed cylindrical phase at the corresponding volume fractions, respectively.

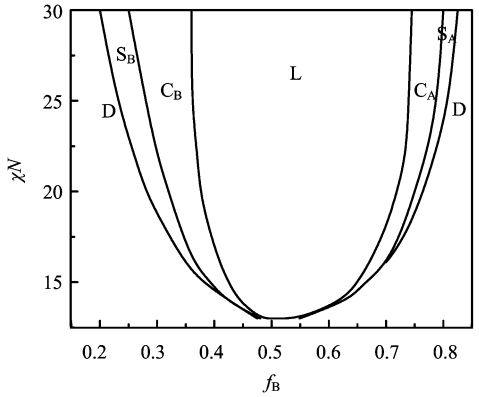

FIG. 3 Phase diagram showing regions of stability for the disordered (D), spheres of B (S_B), hexagonal-packed cylinders of B (C_B), lamellar (L), hexagonal-packed cylinders of A (C_A), and spheres of A (S_A) phases for Y copolymer system.

The strong segregation limit (SSL) behavior of Y block copolymer studied in this paper was explored in the mean-field calculations by Milner [15]. Milner used a simple calculation to determine the center of the lamellar phase in a melt of Y polymer. It was found that the B graft component volume fraction is f_B=2/3 in an A_2B block copolymer to produce a flat preferred curvature. The analogous absence of a preferred curvature for symmetric diblock architecture occurs at f_B=1/2, revealing the shift of the center of the phase diagram due to architecture alone. In this work, similar boundary shifts are shown in the two diagrams given in Fig.3 and Fig.4. In order to understand these shifts of phase boundaries, we compare the A_2B block copolymer with a corresponding linear diblock copolymer which is different in molecular architecture but with the same molecular weight and composition [26,27]. The two short A blocks (Fig.5(b)) are more highly stretched (Fig.5 (a)) and are twice as long as the single A block. The higher stretching of the two A arms can be partially alleviated by allowing the interface to curve away from them (Fig.5(c)); thus multiple arms of block type A at a single junction result in an enhanced preference when these arms reside on the convex side of the interface. We consider that this preference causes the shifts of phase boundaries to higher B block volume fraction in the morphology diagram.

Moreover, as the range of f_B for which each mi-

ISSN 1003-7713/DOI:10.1360/cjcp2007.20(1).43.5

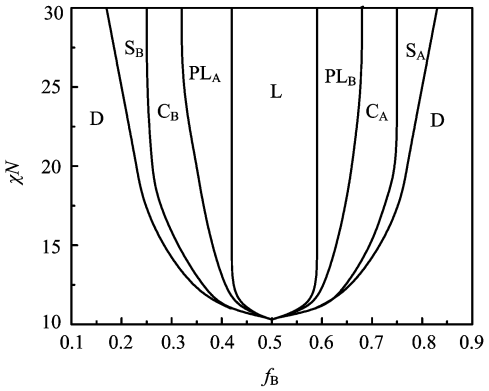

FIG. 4 Phase diagram showing regions of stability for the disordered (D), spheres of B (S_B), hexagonal-packed cylinders of B (C_B), perforated lamellar of A (PL_A), lamellar (L), perforated lamellar of B (PL_B), hexagonal-packed cylinders of A (C_A), and spheres of A (S_A) phases for diblock copolymer system.

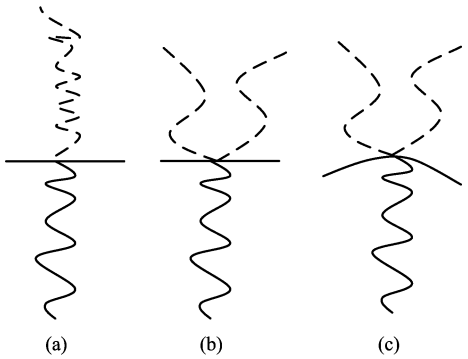

FIG. 5 Schematic diagram of A-B junction points on an interface for (a) AB linear diblock copolymer; (b) A_2B block copolymer with a trifunctional branch point at a flat interface; (c) A_2B block copolymer with a trifunctional branch point at a curved interface.

crostructure occurs is concerned, we find that the range of f_B for which lamellar phase occurs is widened to some degree. The widening is meaningful in applications [28,29] but the mechanism of this change is not understood. In a variety of potential applications, for example, microphases used as semipermeable membranes or templates, suggest an approach for designing copolymers disposed to obtain lamellar phase with a relatively larger scale volume fraction of interior species. In Fig.3, we can also find that the symmetry of the phase diagram is destroyed in the asymmetric Y copolymer and the ranges of f_B, for which S_A and C_A are formed, are much narrower than the ranges of f_B for which S_B and C_B are formed.

For both diblock copolymer system and A_2B copolymer system, the lamellar structure was discovered at volume fraction f_B=0.5 with χN=20 and hexagonal cylinder structure was found at f_B=0.72 with χN=18. We found that the cylinder and lamellar phases discovered in A_2B copolymer are similar to those phases in the diblock copolymer. In the interest of a more accurate comparison, we give the density distribution of A block in one dimension for two systems at f_B=0.5, (shown as Fig.6) and calculate the intervals between two layers. The intervals between two lamellas, in diblock copolymer and A_2B copolymer, are both equal to 12.014, indicating the same thicknesses of layer in the two systems. The same thing occurs when we calculate the intervals between two cylinders of hexagonal cylindrical structure for the two systems at f_B=0.72 with χN=18.

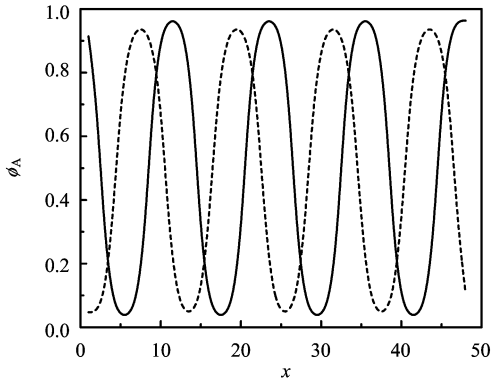

FIG. 6 The density distribution of the A block segment. The solid line represents density distribution of A block in diblock copolymer. The dashed line is the density distribution of A block in Y copolymer system.

IV. CONCLUSION

With the development of new synthesis methods, experimental studies on more complex architectures started emerging. This in turn inspired new theoretical work into the effect of architectures on morphological behavior. In this paper, we investigate the self-assembly of a A_2B simple graft copolymer by using self-consistent field theory in a 3D space and predicting the functional dependence between morphology and the relative volume fraction of blocks by exploring the volume fraction and the Flory-Huggins χ parameter spaces. This morphological study of A_2B block copolymer yields two important results. First, the change that happened in chain architecture causes sufficient shifts of order-order transition lines to higher B block volume fractions in the phase diagram. Second, our results confirm that the architectural asymmetry of the A_2B block copolymer results in a large asymmetry relative to volume fraction in the equilibrium phase behavior. These results indicate how molecular architecture provides another controllable parameter besides the respective block volume fractions to manipulate the morphology of self-assembly. Furthermore, the research on this single-graft block copolymer is helpful in understanding the mor-

ISSN 1003-7713/DOI:10.1360/cjcp2007.20(1).43.5

phological behavior of complex architectures such as π-shaped and H-shaped double graft copolymers.

[1] D. J. Kinning, E. L. Thomas and J. Ottino, Macromolecules **20**, 1129 (1987).
[2] J. D. Vavasour and M. D. Whitmore, Macromolecules **25**, 5477 (1992).
[3] G. Holden, N. R. Legge, R. P. Quirk and H. E. Schroeder, *Thermoplastic Elastomers*, 2nd ed.; NewYork: Hanser Publishers, (1996).
[4] S. H. Yang, J. H. Jin and G. Li, Chin. J. Chem. Phys. **17**, 577 (2004).
[5] H. R. Cong, X. F. Bian, H. Li and L. Wang, Chin. J. Chem. Phys. **15**, 153 (2002).
[6] F. Li, R. J. Gaymans, S. H. Yang and J. M. Jiang, Chin. J. Chem. Phys. **17**, 105 (2004).
[7] E. Helfand, Z. R. Wasserman, *In Developments in Block Copolymers*-1, I. Goodman, Eds. New York: Applied Science, (1982).
[8] L. Leibler, Macromolecules **13**, 1602 (1980).
[9] A. N. Semenov, Sov. Phys. JETP **61**, 733 (1985).
[10] M. W. Matsen and M. Schick, Phys. Rev. Lett. **72**, 2660 (1994).
[11] M. W. Matsen and F. S. Bates, J. Chem. Phys. **106**, 2436 (1997).
[12] C. A. Tyler and D. C. Morse, Phys. Rev. Lett. **94**, 208302 (2005).
[13] P. Tang, F. Qiu, H. D. Zhang and Y. L. Yang, J. Phys. Chem. B **108**, 8434 (2004).
[14] M. W. Matsen and M. Schick, Macromolecules **27**, 6761 (1994).
[15] S. T. Milner, Macromolecules **27**, 2333 (1994).
[16] A. Frischknecht and G. H. Fredrickson, Macromolecules **32**, 6831 (1999).
[17] E. Helfand, J. Chem. Phys. **62**, 999 (1975).
[18] S. F. Edwards, Proc. Phys. Soc. **85**, 613 (1965).
[19] S. W. Sides and G. H. Fredrickson, Polymer **44**, 5859 (2003).
[20] F. Drolet and G. H. Fredrickson, Macromolecules **34**, 5317 (2001).
[21] F. Drolet and G. H. Fredrickson, Phys. Rev. Lett. **83**, 4217 (1999).
[22] W. H. Press, B. P. Flannery, S. A. Teukolsky and W. T. Vetterling, *Numerical Recipes*, Cambridge: Cambridge University Press, (1989).
[23] D. A. Hajduk, H. Takenouchi, M. A. Hillmyer, F. S. Bates, M. E. Vigild and K. Almdal, Macromolecules **30**, 3795 (1997).
[24] D. A. Hajduk, R. M. Ho, M. A. Hillmyer, *et al.* J. Phy. Chem. B **102**, 1356 (1998).
[25] D. J. Pochan, S. P. Gido, S. Pispas, J. W. Mays, *et al.* Macromolecules **29**, 5091 (1996).
[26] C. Lee, S. P. Gido, Y. Poulos and N. Hadjichristidis, *et al.* Polymer **19**, 4631 (1998).
[27] C. Lee, S. P. Gido, Y. Poulos, *et al.* J. Chem. Phys. **107**, 6460 (1997).
[28] Y. C. Chen, G. X. Liu and X. M. Ren, Chin. J. Chem. Phys. **15**, 288 (2002).
[29] P. Liu, Q. J. Xue, J. Tian and W. M. Liu, Chin. J. Chem. Phys. **16**, 481 (2003).

ISSN 1003-7713/DOI:10.1360/cjcp2007.20(1).43.5